water

MDPI

Article

Exploring the Cumulative Selectivity of Polycyclic Aromatic Hydrocarbons in Phytoplankton, Water, and Sediment in Typical Urban Water Bodies

Liling Xia [1,2,*], Zhenhua Zhao [2,*], Zihan Lang [3], Zhirui Qin [2] and Yuelong Zhu [4]

[1] School of Computer & Software, Nanjing Vocational University of Industry Technology, Nanjing 210016, China
[2] Key Laboratory of Integrated Regulation and Resource Development on Shallow Lake of Ministry of Education, College of Environment, Hohai University, Nanjing 210098, China
[3] College of Resources and Environment, Shandong Agricultural University, Taian 271018, China
[4] College of Computer and Information, Hohai University, Nanjing 210098, China
* Correspondence: xiall@niit.edu.cn (L.X.); zzh4000@hhu.edu.cn (Z.Z.); Tel.: +86-13505199648 (L.X.)

Abstract: To understand the interactions among eutrophication, algal bloom, and POPs (persistent organic pollutants) in freshwater ecosystems, the cumulative selectivity of PAHs (polycyclic aromatic hydrocarbons) in phytoplankton, water, and sediment with different eutrophication level waters were identified in a typical plain river network region located in Nanjing City. Results showed that a total of 33 algal species belonging to 27 genera and 4 phyla were identified in 15 sites of urban water bodies, and most of them belonged to the type Cyanobacteria–Bacillariophyta. The eutrophication level of these rivers and lakes led to the sample site specificity of algal composition and abundance. The planktonic algae mainly accumulated the 2-ring and 3-ring PAHs, and the sediment mainly enriched the high-ring PAHs. However, the enrichment capacity of planktonic algae on PAHs was much higher than that of sediment. Cyanophyta and some species of Bacillariophyta and Chlorophyta in mesotrophic (βm) and meso-eutrophic water bodies ($\beta\alpha$m) preferentially accumulated lower-ring PAHs (naphthalene, acenaphthylene, and phenanthrene). Some other specific algae species, such as Euglenophyta, some species of Bacillariophyta, and most Chlorophyta in mesotrophic and moderate eutrophic water bodies, had strong capacities to enrich high-ring PAHs subsuming benzo[a]anthracene, chrysene, and anthracene. The eutrophication level of water bodies affected the cumulative selectivity of PAHs by shaping the site specificity of phytoplankton composition, which may be related to water quality, sediment characteristics, phytoplankton composition, and the algal cell walls.

Keywords: planktonic algae; PAHs; ecological contribution; eutrophication level; bioaccumulation

Citation: Xia, L.; Zhao, Z.; Lang, Z.; Qin, Z.; Zhu, Y. Exploring the Cumulative Selectivity of Polycyclic Aromatic Hydrocarbons in Phytoplankton, Water, and Sediment in Typical Urban Water Bodies. *Water* **2022**, *14*, 3145. https://doi.org/10.3390/w14193145

Received: 20 August 2022
Accepted: 30 September 2022
Published: 6 October 2022

1. Introduction

Polycyclic aromatic hydrocarbons (PAHs) refer to compounds with two or more benzene rings arranged by linear, angular, and cluster forms, which possess high melting and boiling points, strong hydrophobicity, low vapor pressure, and a large *K*ow (the octanol/water partition coefficient). They can exist in natural environments persistently and have carcinogenic, teratogenic, and mutant characteristics [1].

Planktonic algae as a good biosorbent have a strong bioenrichment ability to PAHs [2–7]. The PAHs accumulated in planktonic algae are affected by a series of factors which are composed of pH value, temperature, ion intensity, molecular structure and initial concentration of organic compounds, and metabolic types of microorganisms [8–14]. Mailhot et al. [11] indicated a positive correlation between the enrichment coefficient of planktonic algae and the hydrophobicity of PAHs. Koelmans et al. [15] verified the non-linear relations between the enrichment coefficient of planktonic algae and the *K*ow of organic micropollutants through simulating experiments in the lab. Martinez et al. [16] demonstrated that

the difference in PAHs enrichment was mainly caused by the difference in hydrophobic lipids in the cell wall of algae. Yan et al. [2] studied the enrichment of PAHs by *Chlorella protothecoides* with different metabolic types (autotrophic and heterotrophic), and the results showed that heterotrophic *Chlorella protothecoides* showed stronger enrichment capacity than the autotrophic ones. Soto et al. [17] found that *Chlamydomonas* grew in an airtight tube equipped with a substrate containing 30 $mg \cdot L^{-1}$ naphthalene, which could enrich naphthalene until up to a high concentration at 7 d. Subsequently, naphthalene could be quickly released from *Chlamydomonas* after it is transferred to a pure substrate. Lei et al. [18] found that two kinds of freshwater microalgae, *Selenastrum capricornutum* and *Chlorella vulgaris*, were able to remove 48~78% of fluoranthene and pyrene in the culture solution. Kris et al. [19] showed that the concentration level of benzopyrene in brown algae, red algae, green algae, and chara algae was species-specific. Hong et al. [20] indicated that two typical PAHs can be enriched simultaneously by *Skeletonema costatum* (Greville) Cleve and *Nitzschia* sp., and the accumulation and degradation abilities of *Nitzschia* sp. were higher than those of *S. costatum*. The microalgal species also showed comparable or higher efficiency in the removal of the Phe-Fla mixture than Phe or Fla singly, suggesting that the presence of one PAH stimulated the degradation of the other. Chung et al. [21] found that the percentage removals of aqueous Phe by *Sargassum* for all the investigated factors (e.g., initial pH and ionic strength) were in the range of 91.7–98.4%. *Sargassum* is an effective sorbent for removing HOCs (hydrophobic organic compounds) in wastewaters and urban runoffs. Chan et al. [22] found that the removal efficiency of phenanthrene, fluoranthene, and pyrene by *Selenastrum capricornutum* was directly related to the initial cell density, and the optimal density was 1×10^7 cells/mL. The removal rate of the three pollutants was in the order: pyrene > fluoranthene > phenanthrene. Meanwhile, the removal mechanism included an initial adsorption onto the cell walls of both live and dead cells, and the adsorbed PAHs were then absorbed and degraded in live cells only. García et al. [14] found that sorption is an important phenomenon for BaP removal by *Selenastrum capricornutum*; however, biodegradation is the principal means of removing BaP in live cells. Further, most of the BaP removal of *Selenastrum acutus* is due to sorption rather than degradation. Ke et al. [23] found that the presence of metal ions was beneficial to the adsorption of low molecular weight PAHs (Flu and Phe) by algae, which was attributed to metal-induced cell degeneration. However, the presence of metal ions could not affect the absorption of high molecular weight PAHs (Fla, Pyr, and BaP). This conclusion partly confirmed the results of other studies in the same period. Most studies showed that the biosorption efficiency and adsorption capacity of organics decreased due to the shielding effect of heavy metal ions. However, some researchers have found that the presence of heavy metal ions could also improve the adsorption capacity of algae because metal ions played a bridging role between microorganisms and organic matter. Li et al. [24] found that the basal metabolism associated with the growth and proliferation of algal cells could be significantly promoted by bacterial pyrene metabolites, which suggests a close relationship between algae and bacteria in the transformation and ecological effects of toxic contaminants. Luo et al. [25] found that the two light sources (gold and white light irradiation) did not result in significant differences in the biodegradation of the selected PAHs in live algal cells, but white light was more effective in promoting photodegradation than was gold light in dead cells, and dead algal cells most likely acted as a photosensitizer and accelerated the photodegradation of PAHs. Warshawsky et al. [26] showed that algae are important in their ability to degrade PAHs, but the degradation is dependent on the dose of light energy emitted and absorbed, the dose of PAHs to which the algae are exposed, the phototoxicity of PAHs and their metabolite(s), and the species and strain of algae involved. All of these factors are important in assessing the degradation and detoxification pathways of recalcitrant PAHs by algae.

The enrichment of PAHs by algae is a complex biochemical process, which is caused by a combination of multiple mechanisms. The enrichment routines are composed of biosorption and active transportation. Of them, biosorption is the main route of algal bioenrichment, which is fast and has nothing to do with metabolism. Meanwhile, dead

cells can also participate in it. Due to cell wall fragmentation, the carboxyl, amino, aldehyde, phosphoryl, and other internal functional groups in the cytoplasm are exposed to environmental media and are easy to bind with organic matter, which makes the dead cells have strong biosorption ability. Research showed that biosorption may promote biodegradation (the bioavailability of PAHs is mainly improved by shortening the distance between pollutants and degrading bacteria, including the attachment of pollutants to planktonic algae biomass and the chemotaxis of algae to pollutants). Compared with biosorption, active transportation contributes little to algal enrichment, and only living cells can participate in it. Active transportation is an active intracellular absorption process that relies on energy transfer, which requires the participation of some specific enzymes, such as glutathione transferase and cytochrome P450, and is also affected by temperature, light, and metabolic inhibitors [27–31].

The enrichment of PAHs by algae is an important route for the physical transfer of poisons, and PAHs could be transferred through food chains at a high level [32]. Meanwhile, PAHs enriched by algae can reduce the direct impact on other organisms, especially humans. However, previous research is concerned more with algae enrichment of PAHs in laboratories rather than in rivers and lakes. In this work, the main purpose was to identify species-specific algae and their cumulative selectivity of PAHs in phytoplankton, water, and sediment in rivers and lakes with different eutrophication levels, so as to provide a technical basis and reference for ecological restoration and management of similar water bodies.

2. Materials and Methods

2.1. Sample Collection and Pretreatment

The samples of water, sediment, and phytoplankton were collected from 15 sampling sites of Qinhuai River and Xuanwu Lake in Nanjing City on 15 October 2021 (Figure 1). The physicochemical environmental parameters, including dissolved oxygen (DO), total nitrogen (TN), ammonia nitrogen (NH_4^+-N), chemical oxygen demand (permanganate index, COD_{Mn}), and chlorophyll a (*Chl-a*), were measured according to the reference of Zhao et al. [33,34]. The PAHs in water samples were extracted with a C18 solid-phase extraction column (Borui Co., Ltd., Tianjin, China) and concentrated with a vacuum rotary evaporator (RE-3000, Yarong Biochemical Instrument Plant, Shanghai, China) for the determination of PAHs concentration with HPLC. The PAHs accumulated by phytoplankton in a 25 L water sample were collected from the concentrated phytoplankton by filtration (passing through a 25# phytoplankton net and a 0.2 μm glass fiber filter, respectively) and ultrasonic extraction method according to the reference of Zhao et al. [33]. The PAHs were analyzed by Agilent1100 HPLC with fluorescence and UV detectors in a gradient program at 0.75 mL/min, and were quantified by using external standard methods according to the references of Zhao et al. [35]. The algae in 1 L water samples were identified and accounted for by the microscopic examination method after being settled out and concentrated to 30 mL. More detailed information can be found in the Supplementary Materials S1.1–S1.6, and Quality Assurance/Quality Control can be found in the Supplementary Materials S1.7.

2.2. Data Analysis

To explore the influence of algae on the partitioning of PAHs among water, sediment, and algae, RDA analyses of phytoplankton species, sampling sites, and residues of PAHs in algae were performed using the CANOCO 5.0 software package (Demo version, Microcomputer Power, Ithaca, NY, USA). The values of phytoplankton abundance/biomass and residual PAHs were normalized by $\log_{10}(x + 1)$-transformation. Because of the potential interaction between algae and PAHs, the data matrix exchange technique was adopted for algal and PAHs data during the RDA analysis. By comparing the RDA ordination results based on this technique, we identified the dominant algal species and residual PAHs in the different sampling sites and determined the ecological contribution and role of phytoplankton to the bioaccumulation of PAHs in the studied rivers and lakes.

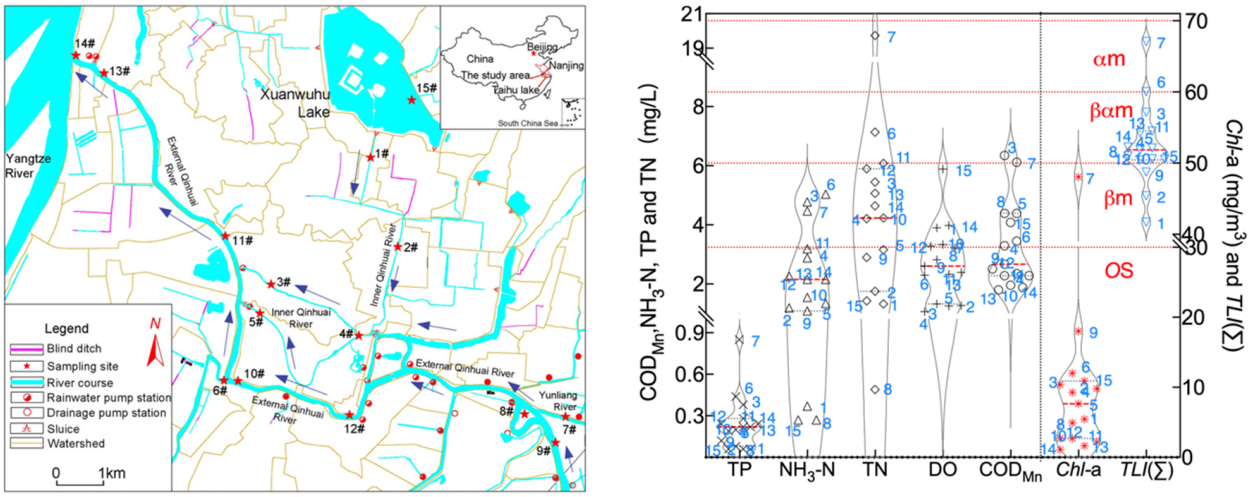

(**A**) (**B**)

Figure 1. Sampling sites (**A**) and the corresponding physicochemical indexes of water samples (**B**) in the study area in Nanjing City, China. Note: (1) The codes for each sampling site are as follows: 1#: Zhenzhu Bridge, 2#:Yixian Bridge, 3#: Wenjin Bridge, 4#: Wenzheng Bridge, 5#: Xiafu Bridge, 6#: Saihong Bridge, 7#: Yunliang River, 8#: Wetland Park, 9#: External Qinhuai River, 10#: Fengtai Bridge, 11#: Hanzhongmen Bridge, 12#: Yuhua Bridge, 13#: Inside the Sancha Estuary, 14#: Outside the Sancha Estuary: 15#: Xuanwu Lake. (2) TLI(∑): comprehensive nutrition state index. (3) os: Oligotrophication refers to a water body that lacks nutrients and contains a large number of species but a small number of aquatic organisms; βm: mesotrophic; βαm: meso-eutrophic; αm: moderate eutrophication.

Given the importance of eutrophication to algae enrichment of PAHs, our study applied a comprehensive nutrition index to evaluate the eutrophication level of water bodies in the research area. This method overcomes the one-sidedness evaluation of eutrophication by a single factor, and takes chlorophyll a, total nitrogen (TN), total phosphorus (TP), and the permanganate index (COD_{Mn}) into account. The comprehensive nutrition status index formula is as follows:

$$TLI(\sum) = \sum_{j=1}^{m} W_i \times TLI(j) \quad (1)$$

where *TLI(∑)* means comprehensive nutritional status index (trophic level index); *TLI(j)* represents the nutrition status index of the *j* parameter; and W_j is the relative weight of the nutrition status index of the *j* parameter.

With *Chl*-a as the reference parameter, the normalized relative weight formula of the *j* parameter is as follows:

$$W_j = \frac{r_{ij}^2}{\sum_{j=1}^{m} r_{ij}^2} \quad (2)$$

where r_{ij} is the correlation coefficient between the *j* parameter and the benchmark parameter *Chl*-a, and *m* is the number of evaluation parameters. The *m* value in our study is 4. The correlation r_{ij} between *Chl*-a, TP, TN, and COD_{Mn} in Chinese river and lake water bodies was 0.84, 0.82, and 0.83, and r_{ij}^2 was 0.7056, 0.6724, and 0.6889, respectively. The comprehensive nutrient index and nutrient status classification of water bodies at different sampling sites were shown in Table 1. The classification criteria of eutrophication level, *TLI(∑)* < 30: oligotrophication (*o*s), refers to a water body that lacks nutrients and contains a large number of species but a small number of aquatic organisms; 30 ≤ *TLI(∑)* ≤ 50: mesotrophication (*ß*m); 50 < *TLI(∑)* ≤60: Meso-eutrophication (*ßα*m); 60 < *TLI(∑)* ≤70: moderate eutrophication (*α*m); 70 < *TLI(∑)*: hypereutrophics (*α-ps* and *ß-ps*) [36].

Table 1. List of algae and their indication function of eutrophication levels.

Code	Genus Name	Eutrophication Level	Algae Abundance	Code	Genus Name	Eutrophication Level	Algae Abundance
Cyanophyta				Euglenophyta			
Cy1	*Oscillatoria*	*α*m	++++	E1	*Euglena*	*p*s, *α*m, *β*m	++
Cy2	*Phormidium*	*p*s	++++	E2	*Phacus*	*β*m, *o*s	+
Cy3	*Merismopedia*	*α*m	+++	Chlorophyta			
Bacillariophyta				C1	*Chlorella*	*p*s, *α*m	++
B1	*Navicula*	*βα*m	+	C2	*Ankistrodesmus*	*α*m, *β*m	++
B2	*Melosira*	*βα*m	+++	C3	*Pandorina*	*β*m, *o*s	++
B3	*Cyclotella*	*βα*m	+	C4	*Coelastrum*	*β*m, *o*s	+
B4	*Stephanodiscus*	*α*m	++	C5	*Actinastrum*	*β*m, *o*s	++
B5	*Tabellaria*	*o*s	+	C6	*Oocystis*	*β*m, *o*s	+
B6	*Fragilaria*	*β*m	+	C7	*Scenedesmus*	*α*m, *β*m	++
B7	*Synedra*	*βα*m	+	C8	*Characium*	*o*s, *β*m	++
B10	*Gyrosigma*	*βα*m	+	C9	*Closterium*	*α*m, *β*m	+
B11	*Gomphonema*	*βα*m	+	C10	*Pediastrum*	*β*m, *o*s	+
B12	*Cymatopleura*	*α*m, *β*m	+	C11	*Schroederia*	*p*s	+
B13	*Stauroneis*	*o*s	+				

Note: eutrophication level: *o*s: oligotrophication; *β*m: mesotrophic; *βα*m: mesotrophic-eutrophication; *α*m: moderate eutrophic; *p*s: hypertrophic type [37]. Algae abundance: +, 0–10; ++, 10–50; +++, 50–100; ++++, more than 100; unit, 10^4 cells per liter.

3. Results

3.1. Characteristics of Phytoplankton Community Composition in Autumn

A total of 33 species, 27 genera, and 4 phyla of phytoplankton were detected in rivers and lakes in the studied area, which were mainly composed of Cyanophyta (3 species, 3 genera), Bacillariophyta (15 species, 11 genera), Euglenophyta (3 species, 2 genera), and Chlorophyta (12 species, 11 genera). *Chondria* dominated the Cyanophyta, accounting for 74.61% of the total number of Cyanophyta. Further, 68.54% of the Bacillariophyta was *Melosira*. The number of phytoplankton communities in the study area ranged from 44.76 × 10^4 to 527.14 × 10^4 cells/L, and the mean value was 221.51 × 10^4 cells/L. The abundance of phytoplankton was in the order: Cyanophyta (92.0 × 10^4 cells/L, 41.5%) > Bacillariophyta (81.20 × 10^4 cells/L, 36.7%) > Euglenophyta (27.0 × 10^4 cells/L, 12.2%) > Chlorophyta (21.20 × 10^4 cells/L, 9.6%). Cyanophyta and Bacillariophyta occupied 78.19% of total phytoplankton. Thus, the study area belonged to the type Cyanobacteria–Bacillariophyta in autumn. The codes of phytoplankton and their relative abundance and the indication function of eutrophication levels are listed in Table 1.

The relatively large number of phytoplankton observed in the sample sites included: Outside the Sancha Estuary (527.14 × 10^4 cells/L), Hanzhongmen Bridge (420.32 × 10^4 cells/L), Xiafu Bridge (292.72 × 10^4 cells/L), Yuhua Bridge (277.48 × 10^4 cells/L), and Inside the Sancha Estuary (264.53 × 10^4 cells/L). Meanwhile, a relatively small abundance of phytoplankton was detected in three sample sites—Yixian Bridge (44.76 × 10^4 cells/L), the upper reaches of Qinhuai River (55.99 × 10^4 cells/L), and Xuanwu Lake (76.99 × 10^4 cells/L)—which was much lower than the mean value. Thus, more phytoplankton was distributed in the External Qinhuai River and in the south of the Internal Qinhuai River. Meanwhile, the abundance of phytoplankton in the External Qinhuai River increased from the upper reaches to the lower reaches (Figure 2). The spatial distribution difference of algal abundance and composition may be related to the water flow velocity and eutrophication degree at different sampling points. Due to the sluice controlled stagnant flow in the study area, the water flow speed of rivers and lakes is very slow (about 0.02 m/s) in Xuanwu Lake and the Internal Qinhuai River, and the flow rates of the External Qinhuai River (sites 9#–13#) and Yangze River (14# site: Outside the Sancha Estuary) are more than those of Xuanwu Lake and Internal Qinhuai River. According to the report of Zhang et al. [38], the flow rate significantly inhibited the growth of phytoplankton and dramatically shifted the phytoplankton composition and enhanced the inter-relationships among environmental variables, and the effect of the flow

rate on phytoplankton is interlinked with many other environmental variables. Similar results have been obtained by Li et al. [39].

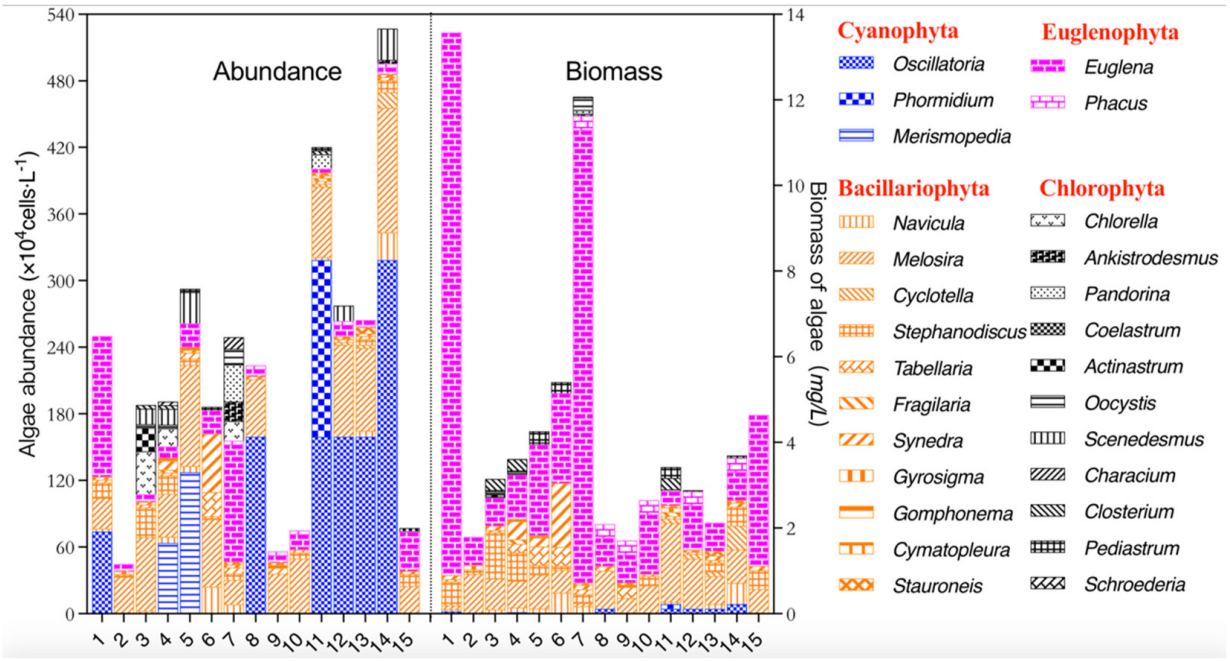

Figure 2. The composition characteristics of algae abundance and biomass in different sampling sites. Note: The codes for each sampling site are shown in Figure 1.

However, the algal biomass showed different spatial distribution characteristics, which may be related to the different weights of individual algal bodies of different algal species.

3.2. Residual Characteristics of PAHs in Phytoplankton, Water, and Sediment

The mean residual concentration of ∑PAHs in phytoplankton was 16,373.6 ng/g. Among these sample sites, the maximum concentration of ∑PAHs in Yixian Bridge was 35,171.9 ng/g, followed by the Inside the Sancha Estuary, Fengtai Bridge, Wetland Park, Yuhua Bridge, Xuanwu Lake, the Outside the Sancha Estuary, Wenjin Bridge, and Xiafu Bridge. The minimum concentration of ∑PAHs in Zhenzhu Bridge was only 1467.2 ng/g, which was approximately 1/24 of the maximum concentration. The PAHs residual components of phytoplankton samples in this region were mainly 2- and 3-ring PAHs, accounting for 99.6% of the total residual amount on average, while the residual concentration of 4-ring PAHs was very low, accounting for only 0.36%. Even 5- or 6-ring PAHs were not detected in phytoplankton (Figure 3A). The eutrophication level of these rivers and lakes led to the sample site specificity of algal composition and abundance. The planktonic algae mainly accumulated PAHs with two and three rings, and the sediment mainly enriched the high-ring PAHs. However, the enrichment capacity of planktonic algae on PAHs was much higher than that of sediment.

From Figure 3B, we found that there was a very poor correlation between the concentrations of ∑PAHs in water and phytoplankton samples (R^2 = 0.033, p = 0.5166). This may be because there are many factors influencing the adsorption of PAHs by phytoplankton, such as the cell structure of algae, the type and structure of PAHs, etc. [8–14]. In addition to the physical and chemical properties and hydrological conditions of each sampling site were different, and the composition and abundance of the algal community were also different, so the concentrations of ∑PAHs between the water and phytoplankton had no obvious correlation. However, there was a significant negative correlation between the concentrations of PAHs in sediments and that of algae (R^2 = 0.4149, p = 0.0175), indicating a direct competitive relationship with PAH accumulation (Figure 3B).

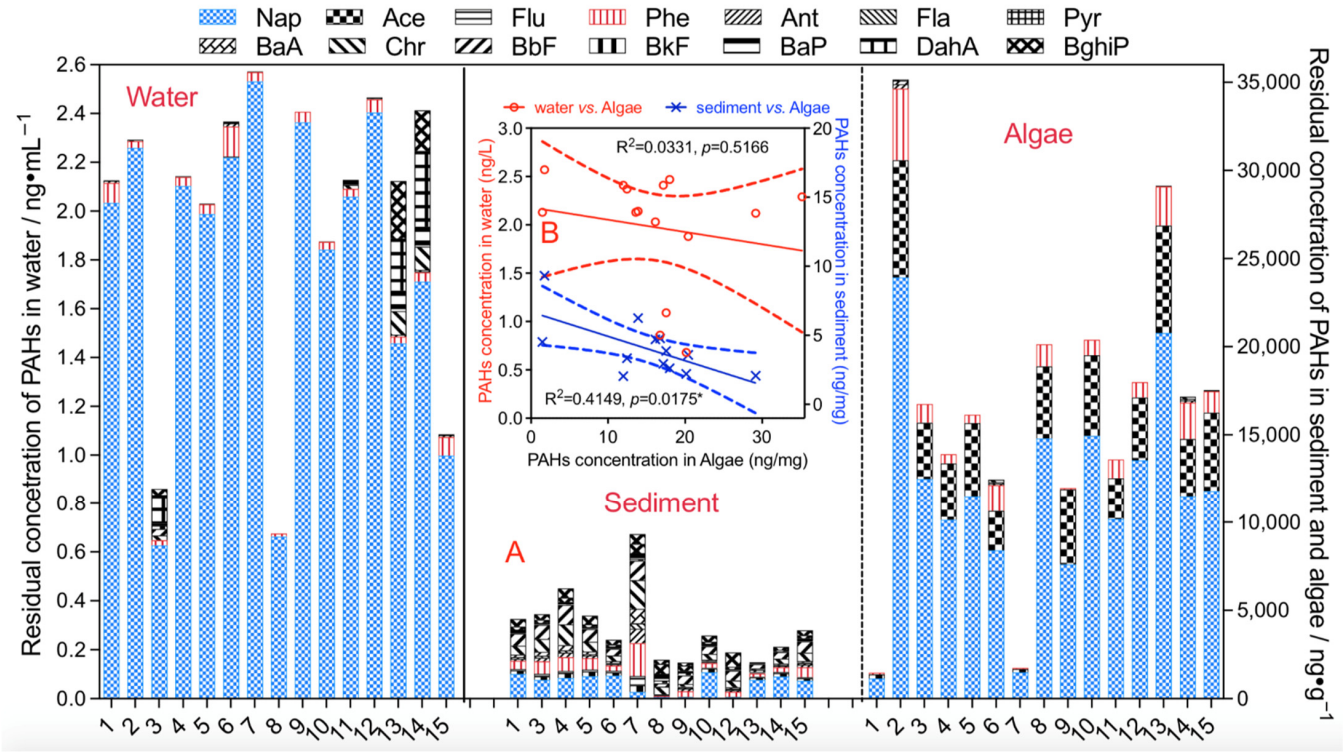

Figure 3. The residual characteristics of PAHs in water, sediment, and algae (**A**) and the correlation of PAHs concentration among algae, water, and sediment (**B**). Note: naphthalene (Nap), phenanthrene (Phe), anthracene (Ant), fluorene (Flu), fluoranthene (Fla), pyrene (Pyr), acenaphthylene (Ace), chrysene (Chr), benzo[a]anthracene (BaA), benzo[b]fluoranthene (BbF), benzo[k]fluoranthene (BkF), benzo[a]pyrene (BaP), dibenzo[a,h]anthracene (DahA), and benzo[g,h,i]perylene (BghiP). *: linear correlation is significant at the 0.0175 level.

3.3. Relationship Analysis between Phytoplankton Community and Residual PAHs

3.3.1. Correlation Analysis

Figure 4 shows the relationship between PAHs and phytoplankton biomass based on Pearson correlation analysis. The results showed that there was an extremely significant positive correlation between Nap, Ace, and Phe ($p < 0.01$). Meanwhile, Phe was positively correlated with Ant, BaA, and Chr ($p < 0.01$). Nap and Ace showed a significant negative correlation with E1 ($p < 0.05$), while Ace showed a significant negative correlation with E1 and C3 and a significant positive correlation with C4 ($p < 0.05$). In addition, Cy3, B2, B11, C7, and C10 also showed a high positive correlation with Nap and Ace. For Phe, B1 was significantly positively correlated with Phe ($p < 0.05$), and Cy1, B2, B3, B7, and B10 were also high positively correlated with Phe. For Ant, BaA, and Chr, B1 and B7 showed significant and extremely significant positive correlations with them ($p < 0.05$ or <0.01). The relationship between phytoplankton abundance and PAHs showed similar results, which are shown in Figure S1 in the Supplementary Materials. These results indicated that these algae played an important role in the absorption and degradation of PAHs.

3.3.2. Redundancy Analysis (RDA)

The structure of the cell walls and the surface characteristics of phytoplankton determine their enrichment efficiency and selectivity on pollutants, and the physicochemical properties of water bodies also affect the phytoplankton composition and their enrichment ability. In our study, CANOCO 5.0 was applied to explore the effect of phytoplankton on the occurrence of PAHs in water. For the first RDA ordination (algae vs. PAHs, Figure 5A), phytoplankton abundance data represented the species matrix and the residues of PAHs in algae represented the environmental matrix. The second RDA ordination reversed

these data matrices (PAHs vs. algae, Figure 5B). The codes for each sampling site and for phytoplankton were exhibited in Figure 1 and Table 1.

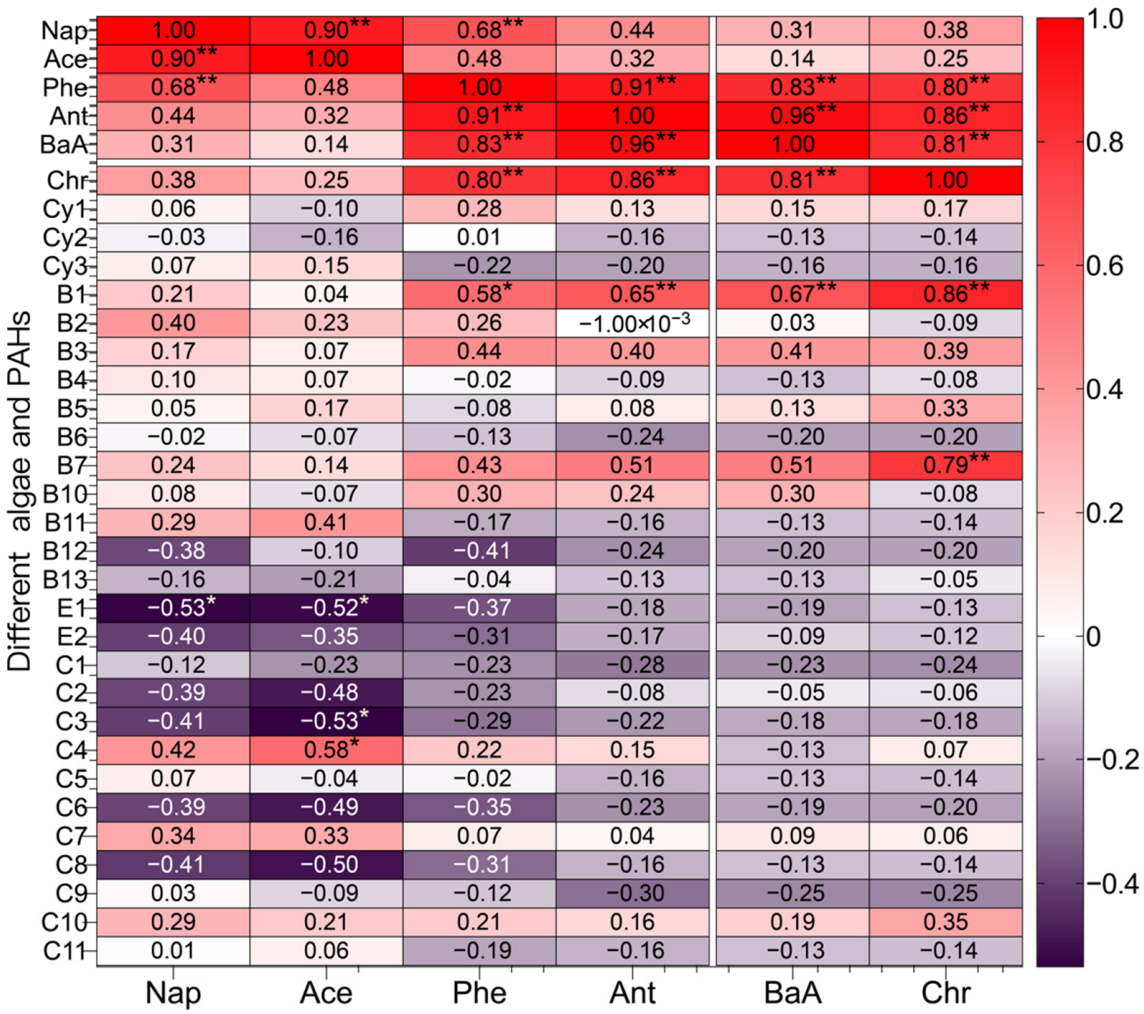

Figure 4. The Pearson correlation analysis between PAHs concentration and algae biomass. Note: (1) **: Correlation is significant at the 0.01 level (2-tailed); *: correlation is significant at the 0.05 level (2-tailed). (2) Naphthalene (Nap), acenaphthylene (Ace), phenanthrene (Phe), anthracene (Ant), benzo[a]anthracene (BaA), chrysene (Chr). (3) The codes of phytoplankton are listed in Table 1.

When phytoplankton abundance data acted as the species matrix and the residues of PAHs as the environmental matrix, the eigenvalues of the first two species axes were 0.210 and 0.118, and the total eigenvalue was 1.000 (Table 2). The first two species axes explained 71.30% of the total information amount. The correlation coefficients between the first two species axes (phytoplankton abundance) and the first two environmental axes (PAHs) were 0.8212 and 0.8858, respectively. The correlation coefficient of the first two species ordination axes and of the first two environmental axes (PAHs) were 0.1298 and 0.000 (indicating little correlation), respectively. When we reversed these data matrices (Figure 5B), the residues of PAHs acted as the species matrix and the phytoplankton abundance data as the environmental matrix. The eigenvalues of the first two species axes were 0.6080 and 0.3259 (Table 2), respectively, explained 93.39% of the total information amount. The correlation coefficients between the first two species axes (PAHs) and the first two environmental axes (phytoplankton abundance) were all 1.000, respectively. The correlation coefficients of the first two species ordination axes and of the first two environmental axes (PAHs) were all 0.000. These RDA results suggested that the ordination could reflect the exact relationship between phytoplankton species and the residues of PAHs.

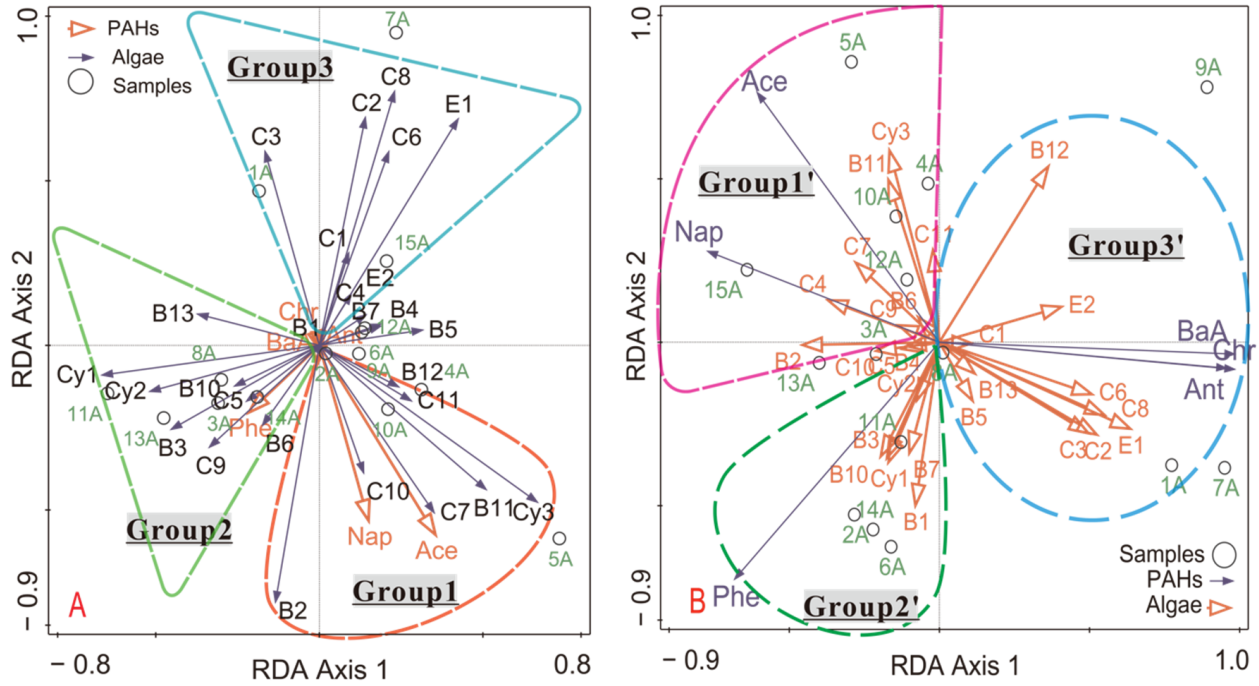

Figure 5. Redundancy analysis (RDA) ordination tri-plot of algae species, sampling sites, and PAHs residues in algae. (**A**) Ordination results when the algae abundance acts as the species matrix and residual PAHs concentrations represent the environmental matrix. The data matrices in (**B**) are opposite those in (**A**). Circles symbol is the sample sites; the arrows are PAHs in (**A**) or the species of algae in (**B**). The length of the arrow corresponds to the importance of the variable.

Table 2. Eigenvalues for RDA axis and the cumulative percentage variance.

Species Matrix vs. Environmental Matrix	Ordination Axes	AX1	AX2	AX3	AX4	Total Variance
Algae vs. PAHs	Eigenvalues	0.210	0.118	0.220	0.129	1.000
	Cumulative percentage variance of fitted response data	45.70	71.30	71.80	73.60	
PAHs vs. algae	Eigenvalues	0.608	0.3259	0.0521	0.0122	1.000
	Cumulative percentage variance of fitted response data	60.8	93.39	98.6	99.83	

Table 3 shows that in the first RDA ordination (algae vs. PAHs), Nap and Ace represented a positive correlation with the first species ordination axis, and the algae including Cy3 (correlation coefficient r = 0.6662), B11 (0.5094), B12 (0.2422), C4 (0.1423), C7 (0.3507), C10 (0.1354), and C11 (0.2808) were also positively correlated with the first ordination axis. This showed that Nap and Ace affected these Algae more. Phe represented a negative correlation with the first species ordination axis, and the corresponding algae including Cy1 (−0.6637), Cy2 (−0.5175), B3 (−0.4524), B6 (−0.1734), B10 (−0.2584), B13 (−0.3717), C5 (−0.2220), and C9 (−0.3358) also showed a negative correlation, which indicated that these algae may have an effect on the accumulation of Phe. BaA, Chr, and Ant were not significantly correlated with the first two species axes in the first kind of RDA analysis. In the second kind of RDA analysis (PAHs vs. algae), these PAHs were positively correlated with the first species ordination axis (r = 0.9559–0.9831), and the corresponding algae consisting of B5 (0.1103), B12 (0.3625), B13 (0.1176), E1 (0.6355), E2 (0.4065), C1 (0.1076), C2 (0.5239), C3 (0.4964), C6 (0.5077), and C8 (0.5496) were also positively correlated with the

first ordination axis. This showed that these algae had important effects on the adsorption and accumulation of these three types of PAHs. In the second RDA analysis, Nap and Ace were significantly positively correlated with the second species ordination axis, and the algae that could have a significant impact on PAHs accumulation was similar to the results of the first RDA analysis. Phe was highly negatively correlated with the first two species axes in the second RDA analysis. The other two algae, B1 and B7, also presented significant effects, but B6, B13, and C9 were excluded. The above results showed that when the matrix exchange technique was used to discuss the interaction of the two kinds of species (phytoplankton and PAHs) that interacted with each other, the results of the two RDA analyses could be mutually confirmed and supplemented.

Table 3. Correlation coefficients among PAHs, algae, and RDA ordination axes.

	Algae vs. PAHs		**PAHs vs. Algae**	
Axes	**SPEC AX1**	**SPEC AX2**	**SPEC AX1**	**SPEC AX2**
Nap	0.1235	−0.4714	−0.7713	0.2783
Ace	0.2914	−0.5094	−0.6067	0.7643
Phe	−0.1766	−0.1804	−0.6816	−0.7247
Ant	0.0052	−0.0169	0.9831	−0.0828
BaA	−0.007	−0.0548	0.9832	−0.0362
Chr	0.0011	−0.0192	0.9559	−0.0792
Cy1	−0.6637	−0.0902	−0.1693	−0.3668
Cy2	−0.5175	−0.1398	−0.074	−0.1767
Cy3	0.6662	−0.4762	−0.1661	0.5866
B1	0.0056	0.0086	−0.0798	−0.4991
B2	−0.134	−0.7793	−0.4556	−0.0083
B3	−0.4524	−0.255	−0.1951	−0.3489
B4	0.187	0.0642	−0.1098	−0.0116
B5	0.3154	0.0465	0.1103	−0.1785
B6	−0.1734	−0.2423	−0.0702	0.0765
B7	0.1868	0.0579	−0.0999	−0.3387
B10	−0.2584	−0.1233	−0.1745	−0.3535
B11	0.5094	−0.4376	−0.1695	0.4963
B12	0.2422	−0.126	0.3625	0.5375
B13	−0.3717	0.0951	0.1176	−0.0955
E1	0.4241	0.6874	0.6355	−0.2645
E2	0.0978	0.1568	0.4065	0.1085
C1	0.0897	0.2804	0.1076	−0.0033
C2	0.1405	0.6918	0.5239	−0.2825
C3	−0.166	0.5891	0.4964	−0.2784
C4	0.1423	0.0922	−0.3705	0.1283
C5	−0.222	−0.1693	−0.1219	−0.0209
C6	0.2121	0.5879	0.5077	−0.1591
C7	0.3507	−0.5079	−0.2782	0.2434
C8	0.23	0.7712	0.5496	−0.2223
C9	−0.3358	−0.3092	−0.1357	0.052
C10	0.1354	−0.3871	−0.2099	−0.0264
C11	0.2808	−0.1685	−0.0217	0.2809

Note: (1) "Algae vs. PAHs" shows the RDA results in which algae data act as the species variable and PAHs data act as the environment variable. "PAHs vs. algae" shows the RDA results in which PAHs data act as the species variable and algae data act as the environment variable. (2) The data marked with blue color font show the algae have a high correlation with Nap and Ace, the green color font shows the algae have a high correlation with Phe, and the red color font shows the algae have a high correlation with Ant, BaA, and Chr.

The algae, PAHs, and sampling sites could be well divided into three groups (dotted circles in Figure 5), and the components included in groups 1, 2, and 3 (Figure 5A) and in groups 1′, 2′, and 3′ (Figure 5B) were basically consistent, and these results were also showed in Table 3. The predominant algal species and the dominant residual PAHs at different sampling sites were determined from the length of the arrows in Figure 5. The

relationship between residual PAHs, indicator algae, and sampling sites in RDA analysis was summarized in Table 4.

Table 4. Summary about the relationship among residual PAHs, indicator algae, and sampling sites in RDA.

Matrix	Group	PAHs	Algae type	Sample Sites
Algae vs. PAHs	1	Nap, Ace	Cy3, B2, B11, B12, C7,C10, C11, B12	4A, 5A, 10A
	2	Phe	Cy1, Cy2, B1, B3, B6, B10, B13, C5, C9	2A,3A, 8A, 11A, 13A, 14A
	3	BaA, Chr, Ant	B1, B5, B7, E1, E2, C1, C2, C3, C4, C6, C8, B4	1A, 6A, 7A, 9A, 12A, 15A
PAHs vs. algae	1	Nap, Ace	Cy3, B2, B6, B11, C4,C7,C9,C10, C11, B4	4A, 5A, 10A,12A, 15A
	2	Phe	Cy1, Cy2, B1, B3, B7, B10, C5	2A, 3A, 6A, 8A, 11A, 13A,14A
	3	BaA, Chr, Ant	B1, B5, B12, B13, E1, E2, C1, C2, C3, C6, C8	1A, 7A, 9A

Note: Different eutrophication levels indicated by different colors, *o*s: oligotrophication; *ß*m: mesotrophic; *ßα*m: meso-eutrophic; *α*m: moderate eutrophic; *p*s: hypertrophic type.

Group 1/1′ was associated with the algae species with high accumulation capacity or strong influence for/on Nap and Ace, and its typical sites were Wenzheng Bridge (Site 4), Xiafu Bridge (Site 5), and Fengtai Bridge (Site 10), which all belonged to meso-eutrophic water bodies. Group1/1′ consisted primarily of Cyanophyta of *Merismopedia* (Cy3, *α*m), Bacillariophyta of *Melosira* (B2, *βα*m), *Fragilaria* (B6, *β*m), *Gomphonema* (B11, *βα*m), and *Cymatopleura* (B12, *α*m, *β*m), Chlorophyta of *Scenedesmus* (C7, *α*m, *β*m), *Pediastrum* (C10, *β*m, *o*s), and *Schroederia* (C11, *p*s). In which, Cy3, B6, B12, C4, C7, and C10 are the indicator species from mesotrophic to moderate eutrophic water bodies (*ß*m, *ßα*m, *α*m), and C11 is the dominant species of hypertrophic water bodies. This group indicated that these algae, which are indicator species from mesotrophic to moderate eutrophic water bodies [39], had a strong ability to bioaccumulate or strong influence for/on Nap and Ace.

Group 2/2′ was associated with the algae species with a high accumulation capacity or strong influence for/on Phe, and its typical sites were Yixian Bridge (site 2), Wenjin Bridge (site 3), Wetland Park (site 8), Hanzhongmen Bridge (site 11), the Inside the Sancha Estuary (site 13), and the Outside the Sancha Estuary (site 14), which belonged to meso-eutrophic water bodies (*ßα*m), except for Yixian Bridge (site 2, *ß*m). Group 2/2′ mainly included Cyanophyta of *Oscillatoria* (Cy1, *α*m) and *Phormidium* (Cy2, *p*s), Bacillariophyta of *Navicula* (B1, *βα*m), *Cyclotella* (B3, *βα*m), *Fragilaria* (B6, *β*m), *Synedra* (B7, *βα*m), and *Gyrosigma* (B10, *βα*m), and Chlorophyta of *Actinastrum* (C5, *β*m, *o*s) and *Closterium* (C9, *α*m, *β*m). Cy1 and Cy2 are the indicator species of moderate eutrophic and hypertrophic water bodies (*α*m and *p*s), B1, B3, B7, and B10 are the indicator species of meso-eutrophic water bodies (*ßα*m), B6, C5, C9, and B13 are the indicator species of oligotrophic and mesotrophic water bodies (*o*s and *ß*m, *ßα*m, and *α*m), and C11 is the dominant species of hypertrophic water bodies [39]. This grouping suggested that these algae, which are the indicator species from oligotrophic to hypertrophic water bodies, had a strong ability to enrich or strongly influence Phe.

Group 3/3′ was associated with the algae species with high accumulation capacity or strong influence for/on BaA, Chr, and Ant, and the typical sites were Zhenzhu Bridge (site 1, *ß*m), Yunliang River (site 7, *α*m), and the External Qinhuai River (site 9, *ß*m). Group 3/3′ mainly included Bacillariophyta of *Navicula* (B1, *βα*m) and *Tabellaria* (B5, *o*s), Euglenophyta of *Euglena* (E1, *p*s, *α*m, *β*m) and *Phacus* (E2, *β*m, *o*s), Chlorophyta of *Chlorella* (C1, *p*s, *α*m), *Ankistrodesmus* (C2, *α*m, *β*m), *Pandorina* (C3, *β*m, *o*s), *Oocystis* (C6, *β*m, *o*s), and *Characium* (C8, *o*s, *β*m). B1, B7, C1, C2, and E1 are the indicator species of meso-eutrophic (*βα*m) and moderate eutrophic water bodies (*α*m), E2, C3, C4, C6, and C8 are the indicator species of mesotrophic water bodies (*ß*m), and B5 is the indicator species of oligotrophic water bodies (*o*s). This grouping suggested that these algae, which are indicator species from oligotrophic to moderate eutrophic water bodies, had a strong ability to enrich or strong influence on BaA, Chr, and Ant.

3.3.3. Stepwise Multiple Regression Analysis

In order to explore the relationship between PAHs content in algae, algae abundance, and biomass, we carried out the stepwise regression analysis based on the data of algae abundance, algae biomass, and PAHs content in different sample sites (Table 5).

Table 5. Results of stepwise multiple regression between algae abundance/biomass and PAHs content.

Group	PAHs	Algae	Algae Entered	Regression Equation	*R*	*F*	*p*
Group I	Nap	Abu [(1)]	E1,	$C_{Nap} = 40.797 - 0.172 \times E1$	0.533	5.174	0.041
			B12	$C_{Nap} = 43.890 - 0.202 \times E1 - 6.778 \times B12$	0.724	6.609	0.012
			C4	$C_{Nap} = 42.579 - 0.209 \times E1 - 6.244 \times B12 + 5.974 \times C4$	0.832	8.250	0.004
			C11	$C_{Nap} = 42.645 - 0.212 \times E1 - 11.023 \times B12 + 5.980 \times C4 + 7.447 \times C11$	0.913	12.571	0.001
			B11	$C_{Nap} = 41.541 - 0.208 \times E1 - 10.604 \times B12 + 6.272 \times C4 + 7.442 \times C11 + 4.620 \times B11$	0.946	15.374	0.000
		Bio [(2)]	E1, B12, Cy3, C4, B5	$C_{Nap} = 40.068 - 2.123 \times E1 - 595.594 \times B12 + 751.959 \times Cy3 + 13{,}544.526 \times C4 + 19.661 \times B5$	0.964	23.525	0.000
	Ace	Abu	C4,	$C_{Ace} = 10.048 + 3.248 \times C4$	0.583	6.685	0.023
			E1,	$C_{Ace} = 11.195 + 3.464 \times C4 - 0.070 \times E1$	0.809	11.346	0.002
			B11	$C_{Ace} = 11.195 + 3.634 \times C4 - 0.068 \times E1 + 3.136 \times B11$	0.920	20.232	0.000
		Bio	C4, E1, B11	$C_{Ace} = 11.195 + 7268.369 \times C4 - 0.685 \times E1 + 156.789 \times B11$	0.920	20.232	0.000
Group II	Phe	Abu	B1	$C_{Phe} = 2.607 + 0.179 \times B1$	0.575	6.426	0.025
		Bio	B1, B10, C4, C3	$C_{Phe} = 1.710 + 12.401 \times B1 + 41.121 \times B10 + 2379.072 \times C4 - 36.288 \times C3$	0.913	12.472	0.001
Group III	Ant	Abu	B1	$C_{Ant} = 0.027 + 0.015 \times B1$	0.657	9.857	0.008
		Bio	B1	$C_{Ant} = 0.025 + 0.738 \times B1$	0.647	9.345	0.009
	BaA	Abu	B1	$C_{BaA} = 0.005 + 0.013 \times B1$	0.678	11.070	0.005
			B10	$C_{BaA} = -0.032 + 0.015 \times B1 + 0.080 \times B10$	0.815	11.860	0.001
			Cy2	$C_{BaA} = -0.036 + 0.015 \times B1 + 0.164 \times B10 - 0.003 \times Cy2$	0.961	44.868	0.000
			C6	$C_{BaA} = -0.025 + 0.016 \times B1 + 0.160 \times B10 - 0.003 \times Cy2 - 0.008 \times C6$	0.979	57.138	0.000
			Cy3	$C_{BaA} = -0.015 + 0.015 \times B1 + 0.156 \times B10 - 0.003 \times Cy2 - 0.008 \times C6 - 0.001 \times Cy3$	0.987	70.048	0.000
			B13	$C_{BaA} = -0.002 + 0.016 \times B1 + 0.151 \times B10 - 0.002 \times Cy2 - 0.008 \times C6 - 0.001 \times Cy3 - 0.011 \times B13$	0.993	93.543	0.000
			B4	$C_{BaA} = 0.015 + 0.016 \times B1 + 0.146 \times B10 - 0.002 \times Cy2 - 0.007 \times C6 - 0.001 \times Cy3 - 0.014 \times B13 - 0.002 \times B4$	0.996	132.037	0.000
		Bio	B1, B10, Cy2, C6	$C_{BaA} = -0.028 + 0.783 \times B1 + 4.023 \times B10 - 3.826 \times Cy2 - 0.412 \times C6$	0.978	54.740	0.000
	Chr	Abu	B1	$C_{Chr} = -0.018 + 0.023 \times B1$	0.862	37.670	0.000
			B7	$C_{Chr} = -0.015 + 0.015 \times B1 + 0.007 \times B7$	0.924	35.079	0.000
			B3	$C_{Chr} = -0.012 - 0.003 \times B1 + 0.016 \times B7 - 0.034 \times B3$	0.954	36.843	0.000
			B7,B3	$C_{Chr} = -0.014 + 0.015 \times B7 + 0.030 \times B3$	0.953	59.420	0.000
			C4	$C_{Chr} = -0.028 + 0.015 \times B7 + 0.031 \times B3 + 0.048 \times C4$	0.970	58.397	0.000
		Bio	B1, B7, C1, B5	$C_{Chr} = -0.029 + 0.766 \times B1 + 0.349 \times B7 - 11.653 \times C1 - 0.406 \times B5$	0.959	28.535	0.000

Note: [(1)]: Abu refers to "Abundance"; [(2)]: Bio refers to "Biomass".

The PAHs accumulated by algae can also be divided into three groups, which was consistent with the results of RDA analysis. When phytoplankton abundance data acted as the independent variable and PAHs content in algae as the dependent variable, the algae species, which can enter the regression equation of PAHs accumulation amount, suggested their important contribution for PAHs accumulation in algae. From the results of regression equation parameters, the *R* value was generally greater than 0.533, most of them were 0.9 (p = 0.041–0.000) and *F* value was greater than 5.174, suggesting that the fits of the regression equation were good.

Group 1 consisted primarily of Nap, Ace, and Bacillariophyta of B11 (*Gomphonema*), B12 (*Cymatopleura*), Chlorophyta of C4 (*Coelastrum*), C11 (*Schroederia*), and Euglenophyta

of E1 (*Euglena*) based on the regression analysis of algae abundance, and also included Cyanophyta of Cy3 (*Merismopedia*) and Bacillariophyta of B5 based on the regression analysis of algae biomass.

Group 2 mainly included Phe and Bacillariophyta of B1 (*Navicula)* according to the regression analysis of algae abundance, and also included Bacillariophyta of B10 (*Gyrosigma*), Chlorophyta of C4 (*Coelastrum*) and C3 (*Pandorina*) based on the regression analysis of algae biomass.

Group 3 consisted primarily of Ant, BaA, Chr, and Cy2 (*Phormidium*) and Cy3 (*Merismopedia*), Bacillariophyta of B1 (*Navicula*), B3 (*Cyclotella*), B4 (*Stephanodiscus*), B7 (*Synedra*), B10 (*Gyrosigma*), and B13 (*Stauroneis*), and Chlorophyta of C4 (*Coelastrum*) and C6 (*Oocystis*) according to the regression analysis of algae abundance, and also included Chlorophyta of C1 (*Chlorella*) and Bacillariophyta of B5 (*Tabellaria*) based on the regression analysis of algae biomass.

4. Discussion

The research on the coupling relation between eutrophication and hydrophobic organic contaminants (HOCs) in rivers and lakes with different trophic statuses has become a research hotspot. The biological pump, equilibrium partitioning, and the indirect influence of eutrophication (e.g., high pH induced by phytoplankton, and phytoplankton life cycling) play critical roles in the occurrence and fate of HOCs (e.g., PAHs) in different eutrophic level waters [40,41]. Eutrophication-induced regime shifts from macrophytes to phytoplankton dominance had a stronger influence on the burial ability of PAHs with higher hydrophobicity, varying with the dominant primary producers associated with the trophic level index of the water column [42]. Moreover, the rising surface air temperature, the declining wind speed, and the reducing days with precipitation had weakened the ability of Chinese lakes to bury 16 PAHs by 69.2 $\pm$ 9.4% $-$ 85.7 $\pm$ 3.6% from 1951 to 2017. The relative contributions of the climatic variables to the reduced burial ability depended on the properties of the PAHs and lakes [43]. Our study also observed the significant negative correlation between the concentration of PAHs in sediments and that of algae (Figure 3B), which implied that phytoplankton had a stronger influence on the burial ability of PAHs in different trophic status waters.

Planktonic algae are considered a good biosorbent and have a strong bioenrichment ability to PAHs [3,5–7]. The accumulation and removal of PAHs by planktonic algae are affected by a series of factors, such as pH value, temperature, ion intensity, molecular structure and initial concentration of organic compounds, metabolic types of microorganisms, the lipid content and composition of the plankton cells, and eutrophication level [9,11–14,44–49]. The species composition and abundance of phytoplankton vary with the change in environmental conditions and trophic status of rivers and lakes [50]. Cytoderm structures and surface characteristics of algae determine their selectivity and enrichment efficiency for specific contaminants [51]. Tao et al. reported that the cyanobacteria life cycle affected the seasonal occurrence of PAHs in water and sediments, and a high pH induced indirectly by eutrophication decreased the seasonal air–water exchange fluxes of PAHs, and reduced the accumulation of PAHs in surface sediments and the aromaticity of surface sediments [52]. The trophic transfer of the PAHs from phytoplankton to zooplankton increased with phytoplankton biomass and temperature, but decreased with the lake trophic state index. Biomagnification only occurred during phytoplankton bloom periods [40]. The cyanobacterial biomass affected by the trophic status dominated the occurrence of the PAHs in the surface sediments of these lakes. The biomass dilution and biological pump affected the accumulation of the PAHs in phytoplankton and zooplankton, and had a bigger influence on the PAHs with higher hydrophobicity. Both the bioconcentration factors and bioaccumulation factors of the PAHs decreased with the TSI [53].

At the same time, the increasing pollutants' concentrations (e.g., PAHs) negatively affected the phytoplankton abundance, composition, and physiology, including photosyn-

thetic inhibition, DNA damage, reduced gene expression, and oxidative stress [44,54–56]. Othman et al. observed dramatic changes in the phytoplankton community composition and size classes, and smaller cells were more resistant to the highest PAH concentrations. [54]. Sreejith et al. reported that pyrene was found to be more toxic to phytoplankton, picoeukaryotes exhibited higher sensitivity to PAHs than *Synechococcus*, and the populations in the highly oligotrophic northern region of the Red Sea were more tolerant to PAHs [55]. In our research, we also observed the sample site specificity and algal species specificity for the PAHs accumulation in algae due to the difference in eutrophication levels (Figures 2 and 3), and the significant negative correlation between phytoplankton abundance and PAHs residue, which implied that the PAHs had induced adverse effects on these algae.

As shown in Figures 2 and 3, the predominant algal species and dominant residual PAHs in water, sediment, and algae varied significantly across the study area ($p < 0.01$). These differences may have been related to water chemical characteristics and phytoplankton composition (Table 1, Figures 1B and 2). Thus, the residual characteristics of PAHs in water, sediment, and algal samples indicated sample site and algal species specificity. The capacity of algae to accumulate PAHs is influenced by many factors, including the physicochemical properties of water, the type and structure of PAHs, and the algal cell characteristics (e.g., lipid content) and community composition [57]. Due to their lipophilic nature, PAHs tend to accumulate in phytoplankton cells. For example, *Thalassiosira* sp. showed the highest proportion of PAH-sorbed cells (29% and 97% of total abundance for phenanthrene and pyrene, respectively), which may be attributed to its relatively high total lipid content (33.87% dry weight) [44]. Moreover, the changes in the nitrogen status of algae can increase algal lipid content and affect the bioconcentration of hydrophobic organic compounds (HOCs). Bioconcentration factors (BCFs) for several HOCs increased up to nine-fold when the total lipid content of the green algae *Selenastrum capricornutum* increased from 17% to 44% of algal dry weight under nitrogen starvation [58]. It can be seen that the eutrophication level of river and lake waters could indeed affect the distribution characteristics of PAHs in water, sediments, and algae. In our study, the bioconcentration factors (BCF) of PAHs from water to phytoplankton in the study area were calculated, and the linear equation between logBCF and log*Kow* of PAHs showed that the logBCF of different PAHs were basically linearly positively correlated with log*Kow* of PAHs ($R^2 = 0.3866$); however, the BCF of Phe and Chr obviously deviated from the linear trend (Figure 6).

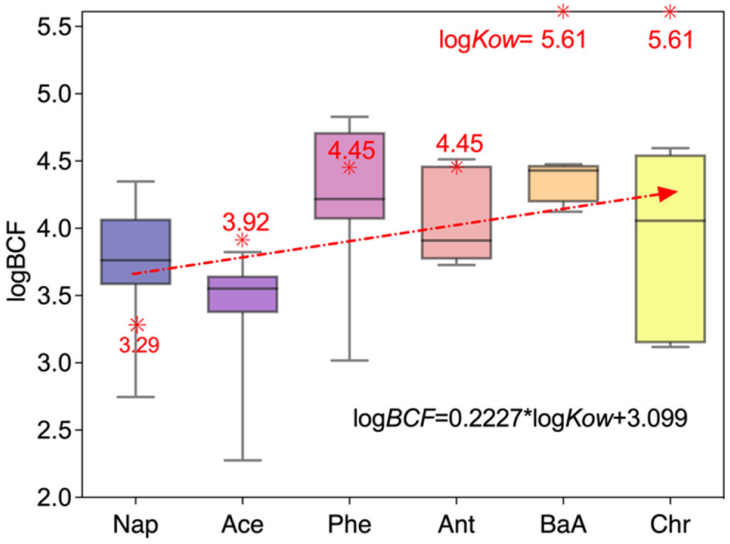

Figure 6. The bioconcentration factors (BCF) of PAHs from water to phytoplankton and the linear equation between logBCF and log*Kow* of PAHs. Note: (1) * and the red text shows the log*Kow* of different PAHs. (2) Naphthalene (Nap), acenaphthylene (Ace), phenanthrene (Phe), anthracene (Ant), benzo[a]anthracene (BaA), and chrysene (Chr).

In this study, using RDA based on the data matrix exchange technique, we found that the eutrophication level of water bodies did affect phytoplankton composition, bioaccumulation of PAHs by phytoplankton, and led to sample site and algal species specificity. Some specific algae species, such as Cyanophyta and some species of Bacillariophyta and Chlorophyta, in mesotrophic (βm) and meso-eutrophic water bodies ($\beta\alpha$m), preferentially accumulated lower-ring PAHs (Nap, Ace, and Phe), and some other specific algae species, such as Euglenophyta, some species of Bacillariophyta, and most of Chlorophyta, in mesotrophic and moderate eutrophic water bodies preferentially accumulated higher-ring PAHs (BaA, Chr, and Ant).

5. Conclusions

The eutrophication level of water bodies did affect phytoplankton composition, bioaccumulation of PAHs by phytoplankton, and led to sample site and algal species specificity. The planktonic algae mainly accumulated the PAHs with two and three rings. Cyanophyta and some species of Bacillariophyta and Chlorophyta in mesotrophic (βm) and meso-eutrophic water bodies ($\beta\alpha$m) preferentially accumulated lower-ring PAHs (Nap, Ace and Phe with 2- and 3-ring PAHs). Some other specific algae species, such as Euglenophyta, some species of Bacillariophyta, and most of Chlorophyta in mesotrophic and moderate eutrophic water bodies, had strong capacities to enrich the BaA, Chr, and Ant with high-ring PAHs. The ecological contribution of phytoplankton on PAHs accumulation may be affected by the eutrophication level of water bodies, phytoplankton composition, and the structure of the PAHs and the algal cell walls.

Supplementary Materials: The following supporting information can be downloaded at: https://www.mdpi.com/article/10.3390/w14193145/s1, Figure S1: The Pearson correlation analysis between PAHs concentration and algae abundance [59–61].

Author Contributions: Conceptualization, methodology, software, validation, formal analysis, investigation, resources, data curation, L.X., Y.Z., Z.Z., Z.Q. and Z.L.; writing—original draft preparation, writing—review and editing, visualization, L.X., Z.Q. and Z.Z.; supervision, Y.Z.; project administration, L.X. and Z.Z.; funding acquisition, L.X. and Z.Z. All authors have read and agreed to the published version of the manuscript.

Funding: This work was supported by the National Natural Science Foundation of China (Grants No. 52070072, 51879080 and 51509129), National Key Research & Development Program of China (No. 2019YFC1804303), Natural Science Foundation of Jiangsu Province, China (BK20171435), a project funded by the Priority Academic Program Development of Jiangsu Higher Education Institutions (PAPD), and the Top-notch Academic Programs Project (TAPP) of Jiangsu Higher Education Institutions the, Key program of Nanjing Institute of Industry Technology (YK14-04-02), and the Outstanding scientific and technological innovation team of Higher Education, 2017 Jiangsu Province (Industrial Big Data Applications, 902050617TD003).

Data Availability Statement: The datasets used and/or analyzed under the current study are available from the corresponding author upon reasonable request.

Conflicts of Interest: The authors declare no conflict of interest.

References

1. Wang, C.; Zhou, S.; Song, J.; Wu, S. Human health risks of polycyclic aromatic hydrocarbons in the urban soils of Nanjing, China. *Sci. Total Environ.* **2018**, *612*, 750–757. [CrossRef] [PubMed]
2. Yan, X.; Yang, Y.; Li, Y.; Sheng, G.; Yan, G. Accumulation and biodegradation of anthracene by *Chlorella protothecoides* under different trophic conditions. *Chin. J. Appl. Ecol.* **2002**, *13*, 145–150.
3. Hung, W.-N.; Chiou, C.T.; Lin, T.-F. Lipid–water partition coefficients and correlations with uptakes by algae of organic compounds. *J. Hazard. Mater.* **2014**, *279*, 197–202. [CrossRef]
4. Watanabe, K.H.; Lin, H.-I.; Bart, H.L.; Martinat, P.; Means, J.C.; Kunas, M.L.; Grimm, D.A. Bayesian estimation of kinetic rate constants in a food-web model of polycyclic aromatic hydrocarbon bioaccumulation. *Ecol. Model.* **2005**, *181*, 229–246. [CrossRef]
5. Koelmans, A.A. Limited Reversibility of Bioconcentration of Hydrophobic Organic Chemicals in Phytoplankton. *Environ. Sci. Technol.* **2014**, *48*, 7341–7348. [CrossRef] [PubMed]

6. Pathak, B.; Gupta, S.; Verma, R. Biosorption and Biodegradation of Polycyclic Aromatic Hydrocarbons (PAHs) by Microalgae. In *Green Adsorbents for Pollutant Removal: Fundamentals and Design*; Crini, G., Lichtfouse, E., Eds.; Springer International Publishing: Cham, Switzerland, 2018; pp. 215–247. [CrossRef]
7. Baghour, M. Algal Degradation of Organic Pollutants. In *Handbook of Ecomaterials*; Martínez, L.M.T., Kharissova, O.V., Kharisov, B.I., Eds.; Springer International Publishing: Cham, Switzerland, 2019; pp. 565–586. [CrossRef]
8. Casserly, D.M.; Davis, E.M.; Downs, T.D.; Guthrie, R.K. Sorption of organics by *Selenastrum capricornutum*. *Water Res.* **1983**, *17*, 1591–1594. [CrossRef]
9. Swackhamer, D.L.; Skoglund, R.S. Bioaccumulation of PCBs by algae: Kinetics versus equilibrium. *Environ. Toxicol. Chem.* **1993**, *12*, 831–838. [CrossRef]
10. Geyer, H.; Viswanathan, R.; Freitag, D.; Korte, F. Relationship between water solubility of organic chemicals and their bioaccumulation by the alga Chlorella. *Chemosphere* **1981**, *10*, 1307–1313. [CrossRef]
11. Mailhot, H. Prediction of Algal Bioaccumulation and Uptake Rate of Nine Organic Compounds by Ten Physicochemical Properties. *Environ. Sci. Technol.* **1987**, *21*, 1009–1013. [CrossRef]
12. Sijm, D.T.H.M.; Middelkoop, J.; Vrisekoop, K. Algal density dependent bioconcentration factors of hydrophobic chemicals. *Chemosphere* **1995**, *31*, 4001–4012. [CrossRef]
13. Fan, C.W.; Reinfelder, J. Phenanthrene accumulation kinetics in marine diatoms. *Environ. Sci. Technol.* **2003**, *37*, 3405–3412. [CrossRef] [PubMed]
14. García de Llasera, M.P.; Olmos-Espejel, J.d.J.; Díaz-Flores, G.; Montaño-Montiel, A. Biodegradation of benzo(a)pyrene by two freshwater microalgae *Selenastrum capricornutum* and *Scenedesmus acutus*: A comparative study useful for bioremediation. *Environ. Sci. Pollut. Res.* **2016**, *23*, 3365–3375. [CrossRef] [PubMed]
15. Koelmans, A.A.; Anzion, S.F.M.; Lijklema, L. Dynamics of Organic Micropollutant Biosorption to Cyanobacteria and Detritus. *Environ. Sci. Technol.* **1995**, *29*, 933–940. [CrossRef] [PubMed]
16. Martínez, F.; Jarillo, J.A.; Orús, M.I. Interactions between trichlorfon and three *Chlorophyceae*. *Bull. Environ. Contam. Toxicol.* **1991**, *46*, 599–605. [CrossRef]
17. Soto, C.; Hellebust, J.A.; Hutchinson, T.C. Effect of naphthaene and aqueous crude oil extracts on the green flagellate *Chlamydomonas angulosa* II. Photosynthesis and the uptake and release of naphthalene. *Can. J. Bot.* **1975**, *53*, 118–126. [CrossRef]
18. Lei, A.-P.; Hu, Z.-L.; Wong, Y.-S.; Tam, N.F.-Y. Removal of fluoranthene and pyrene by different microalgal species. *Bioresour. Technol.* **2007**, *98*, 273–280. [CrossRef]
19. Kirso, U.; Irha, N. Role of algae in fate of carcinogenic polycyclic aromatic hydrocarbons in the aquatic environment. *Ecotoxicol. Environ. Saf.* **1998**, *41*, 83–89. [CrossRef]
20. Hong, Y.-W.; Yuan, D.-X.; Lin, Q.-M.; Yang, T.-L. Accumulation and biodegradation of phenanthrene and fluoranthene by the algae enriched from a mangrove aquatic ecosystem. *Mar. Pollut. Bull.* **2008**, *56*, 1400–1405. [CrossRef]
21. Chung, M.K.; Tsui, M.T.K.; Cheung, K.C.; Tam, N.F.Y.; Wong, M.H. Removal of aqueous phenanthrene by brown seaweed Sargassum hemiphyllum: Sorption-kinetic and equilibrium studies. *Sep. Purif. Technol.* **2007**, *54*, 355–362. [CrossRef]
22. Chan, S.M.N.; Luan, T.; Wong, M.H.; Tam, N.F.Y. Removal and biodegradation of polycyclic aromatic hydrocarbons by *Selenastrum capricornutum*. *Environ. Toxicol. Chem.* **2006**, *25*, 1772–1779. [CrossRef]
23. Ke, L.; Luo, L.; Wang, P.; Luan, T.; Tam, N.F.-Y. Effects of metals on biosorption and biodegradation of mixed polycyclic aromatic hydrocarbons by a freshwater green alga *Selenastrum capricornutum*. *Bioresour. Technol.* **2010**, *101*, 6950–6961. [CrossRef] [PubMed]
24. Li, X.; Cai, F.; Luan, T.; Lin, L.; Chen, B. Pyrene metabolites by bacterium enhancing cell division of green alga *Selenastrum capricornutum*. *Sci. Total Environ.* **2019**, *689*, 287–294. [CrossRef] [PubMed]
25. Luo, L.; Wang, P.; Lin, L.; Luan, T.; Ke, L.; Tam, N.F.Y. Removal and transformation of high molecular weight polycyclic aromatic hydrocarbons in water by live and dead microalgae. *Process Biochem.* **2014**, *49*, 1723–1732. [CrossRef]
26. Warshawsky, D.; Cody, T.; Radike, M.; Reilman, R.; Schumann, B.; LaDow, K.; Schneider, J. Biotransformation of benzo[a]pyrene and other polycyclic aromatic hydrocarbons and heterocyclic analogs by several green algae and other algal species under gold and white light. *Chem. Biol. Interact.* **1995**, *97*, 131–148. [CrossRef]
27. Cerniglia, C.E. Biodegradation of polycyclic aromatic hydrocarbons. *Curr. Opin. Biotechnol.* **1993**, *4*, 331–338. [CrossRef]
28. Semple, K.T.; Cain, R.B.; Schmidt, S. Biodegradation of aromatic compounds by microalgae. *FEMS Microbiol. Lett.* **1999**, *170*, 291–300. [CrossRef]
29. Pflugmacher, S.; Wiencke, C.; Sandermann, H. Activity of phase I and phase II detoxication enzymes in Antarctic and Arctic macroalgae. *Mar. Environ. Res.* **1999**, *48*, 23–36. [CrossRef]
30. Warshawsky, D.; Keenan, T.H.; Reilman, R.; Cody, T.E.; Radike, M.J. Conjugation of benzo[a]pyrene metabolites by freshwater green alga Selenastrum capricornutum. *Chem. Biol. Interact.* **1990**, *74*, 93–105. [CrossRef]
31. Thies, F.; Backhaus, T.; Bossmann, B.; Grimme, L.H. Xenobiotic Biotransformation in Unicellular Green Algae (Involvement of Cytochrome P450 in the Activation and Selectivity of the Pyridazinone Pro-Herbicide Metflurazon). *Plant Physiol.* **1996**, *112*, 361. [CrossRef]
32. Shubert, L.E. *Algae as Ecological Indicators*; Shubert, L.E., Ed.; Academic Press Inc.: London, UK, 1984; p. 434. [CrossRef]
33. Zhao, Z.; Mi, T.; Xia, L.; Yan, W.; Jiang, Y.; Gao, Y. Understanding the patterns and mechanisms of urban water ecosystem degradation: Phytoplankton community structure and water quality in the Qinhuai River, Nanjing City, China. *Environ. Sci. Pollut. Res.* **2013**, *20*, 5003–5012. [CrossRef]

34. APHA. *Standard Methods for the Examination of Water and Wastewater*; American Public Health Association: Washington, DC, USA, 2005.
35. Zhao, Z.; Xia, L.; Jiang, X.; Gao, Y. Effects of water-saving irrigation on the residues and risk of polycyclic aromatic hydrocarbon in paddy field. *Sci. Total Environ.* **2018**, *618*, 736–745. [CrossRef] [PubMed]
36. Wang, J.; Fu, Z.; Qiao, H.; Liu, F. Assessment of eutrophication and water quality in the estuarine area of Lake Wuli, Lake Taihu, China. *Sci. Total Environ.* **2019**, *650*, 1392–1402. [CrossRef] [PubMed]
37. Kuang, Q.; Ma, P.; Hu, Z.; Zhou, G. Study on the evaluation and treatment of lake eutrophication by means of algae biology. *J. Saf. Environ.* **2005**, *5*, 87–91.
38. Zhang, H.; Chen, R.; Li, F.; Chen, L. Effect of flow rate on environmental variables and phytoplankton dynamics: Results from field enclosures. *Chin. J. Oceanol. Limnol.* **2015**, *33*, 430–438. [CrossRef]
39. Li, F.; Zhang, H.; Zhu, Y.; Xiao, Y.; Chen, L. Effect of flow velocity on phytoplankton biomass and composition in a freshwater lake. *Sci. Total Environ.* **2013**, *447*, 64–71. [CrossRef]
40. Tao, Y.; Yu, J.; Liu, X.; Xue, B.; Wang, S. Factors affecting annual occurrence, bioaccumulation, and biomagnification of polycyclic aromatic hydrocarbons in plankton food webs of subtropical eutrophic lakes. *Water Res.* **2018**, *132*, 1–11. [CrossRef] [PubMed]
41. Tao, Y.; Yu, J.; Xue, B.; Yao, S.; Wang, S. Precipitation and temperature drive seasonal variation in bioaccumulation of polycyclic aromatic hydrocarbons in the planktonic food webs of a subtropical shallow eutrophic lake in China. *Sci. Total Environ.* **2017**, *583*, 447–457. [CrossRef]
42. Tao, Y. Eutrophication-induced regime shifts reduced sediment burial ability for polycyclic aromatic hydrocarbons: Evidence from Lake Taihu in China. *Chemosphere* **2021**, *271*, 129709. [CrossRef]
43. Tao, Y.; Zhang, Y.; Cao, J.; Wu, Z.; Yao, S.; Xue, B. Climate change has weakened the ability of Chinese lakes to bury polycyclic aromatic hydrocarbons. *Environ. Pollut.* **2019**, *255*, 113288. [CrossRef]
44. Kottuparambil, S.; Agusti, S. Cell-by-cell estimation of PAH sorption and subsequent toxicity in marine phytoplankton. *Chemosphere* **2020**, *259*, 127487. [CrossRef]
45. Ding, Q.; Gong, X.; Jin, M.; Yao, X.; Zhang, L.; Zhao, Z. The biological pump effects of phytoplankton on the occurrence and benthic bioaccumulation of hydrophobic organic contaminants (HOCs) in a hypereutrophic lake. *Ecotoxicol. Environ. Saf.* **2021**, *213*, 112017. [CrossRef] [PubMed]
46. Wei, P.; Fu, H.; Xu, Z.; Zhu, D.; Qu, X. Prediction of hydrophobic organic compound partition to algal organic matter through the growth cycle of *Microcystis aeruginosa*. *Environ. Pollut.* **2021**, *289*, 117827. [CrossRef] [PubMed]
47. Qiu, Y.-W.; Zeng, E.Y.; Qiu, H.; Yu, K.; Cai, S. Bioconcentration of polybrominated diphenyl ethers and organochlorine pesticides in algae is an important contaminant route to higher trophic levels. *Sci. Total Environ.* **2017**, *579*, 1885–1893. [CrossRef] [PubMed]
48. Szczybelski, A.S.; van den Heuvel-Greve, M.J.; Kampen, T.; Wang, C.; van den Brink, N.W.; Koelmans, A.A. Bioaccumulation of polycyclic aromatic hydrocarbons, polychlorinated biphenyls and hexachlorobenzene by three Arctic benthic species from Kongsfjorden (Svalbard, Norway). *Mar. Pollut. Bull.* **2016**, *112*, 65–74. [CrossRef]
49. Duan, D.; Huang, Y.; Cheng, H.; Ran, Y. Relationship of polycyclic aromatic hydrocarbons with algae-derived organic matter in sediment cores from a subtropical region. *J. Geophys. Res. Biogeosci.* **2015**, *120*, 2243–2255. [CrossRef]
50. She, Z.; Huang, X. *Research Methods of Freshwater Plankton*; Science Press: Beijing, China, 1991.
51. Wallberg, P.; Andersson, A. Determination of adsorbed and absorbed polychlorinated biphenyls (PCBs) in seawater microorganisms. *Mar. Chem.* **1999**, *64*, 287–299. [CrossRef]
52. Tao, Y.; Yu, J.; Lei, G.; Xue, B.; Zhang, F.; Yao, S. Indirect influence of eutrophication on air–water exchange fluxes, sinking fluxes, and occurrence of polycyclic aromatic hydrocarbons. *Water Res.* **2017**, *122*, 512–525. [CrossRef]
53. Tao, Y.; Liu, D. Trophic status affects the distribution of polycyclic aromatic hydrocarbons in the water columns, surface sediments, and plankton of twenty Chinese lakes. *Environ. Pollut.* **2019**, *252*, 666–674. [CrossRef]
54. Ben Othman, H.; Lanouguère, É.; Got, P.; Sakka Hlaili, A.; Leboulanger, C. Structural and functional responses of coastal marine phytoplankton communities to PAH mixtures. *Chemosphere* **2018**, *209*, 908–919. [CrossRef]
55. Kottuparambil, S.; Agusti, S. PAHs sensitivity of picophytoplankton populations in the Red Sea. *Environ. Pollut.* **2018**, *239*, 607–616. [CrossRef]
56. Jaiswal, K.K.; Kumar, V.; Vlaskin, M.S.; Nanda, M. Impact of pyrene (polycyclic aromatic hydrocarbons) pollutant on metabolites and lipid induction in microalgae *Chlorella sorokiniana* (UUIND6) to produce renewable biodiesel. *Chemosphere* **2021**, *285*, 131482. [CrossRef] [PubMed]
57. Stange, K.; Swackhamer, D.L. Factors affecting phytoplankton species-specific differences in accumulation of 40 polychlorinated biphenyls (PCBs). *Environ. Toxicol. Chem.* **1994**, *13*, 1849–1860. [CrossRef]
58. Halling-Sørensen, B.; Nyholm, N.; Kusk, K.O.; Jacobsson, E. Influence of Nitrogen Status on the Bioconcentration of Hydrophobic Organic Compounds to *Selenastrum capricornutum*. *Ecotoxicol. Environ. Saf.* **2000**, *45*, 33–42. [CrossRef] [PubMed]
59. Jiao, X.C.; Xu, F.L.; Dawson, R.; Chen, S.H.; Tao, S. Adsorption and absorption of polycyclic aromatic hydrocarbons to rice roots. *Environ. Pollut.* **2007**, *148*, 230–235. [CrossRef] [PubMed]
60. Javid, H.; Zhao, Z.; Pang, Y.; Xia, L.; Hussain, I.; Jiang, X. Effects of Different Water Seasons on the Residual Characteristics and Ecological Risk of Polycyclic Aromatic Hydrocarbons in Sediments from Changdang Lake, China. *J. Chem.* **2016**, *2016*, 8545816.
61. Tam, N.F.Y.; Ke, L.; Wang, X.H.; Wong, Y.S. Contamination of polycyclic aromatic hydrocarbons in surface sediments of mangrove swamps. *Environ. Pollut.* **2001**, *114*, 255–263. [CrossRef]